

ARTICLES

Viscosity Dependence of the Kinetic Parameters of the Radical Ion Pair in Homogeneous Solution Determined by Optically Detected X- and Ku-Band Electron Spin ResonanceYasutaka Kitahama[†] and Yoshio Sakaguchi*

RIKEN (The Institute of Physical and Chemical Research), 351-0198 Wako, Saitama, Japan

Received: August 15, 2007; In Final Form: October 19, 2007

We investigated the dynamics of the radical ion pairs formed by photoinduced electron-transfer reaction from zinc tetraphenyl porphyrin to 2-methyl-1,4-naphthoquinone in mixtures of 2-propanol and cyclohexanol. By the irradiation of a resonant X- (9.16 GHz) or Ku-band (17.41 GHz) microwave pulse, the time profiles of the transient absorptions was modified and the yields of escaping radical ions decreased. From these experiments, we determined the kinetic parameters of the radical ion pairs at various solvent viscosities. The recombination rates of the singlet pairs were (4 ± 4) , (8 ± 3) , and $(16 \pm 3) \times 10^6 \text{ s}^{-1}$ at 5, 10, and 15 cP, respectively. The escape rates were (1.7 ± 0.2) , (1.4 ± 0.1) , and $(0.9 \pm 0.2) \times 10^6 \text{ s}^{-1}$ at 5, 10, and 15 cP, respectively. The viscosity dependence of the kinetic parameters was followed by the simple continuum diffusion model.

Introduction

External magnetic field and resonant microwave (MW) influence photochemical reactions via radical pairs (RPs) by suppressing or promoting the transition among four spin states of RPs, i.e., singlet and three triplet sublevels.^{1,2} These phenomena are called magnetic field effect (MFE) and reaction yield detected magnetic resonance (RYDMR), respectively. The optically-detected electron spin resonance (ODESR), a variation of RYDMR, using a short MW pulse and a nanosecond time-resolved optical absorption has been used to observe directly the reaction dynamics of RPs.^{3,4} The resonant MW pulse induces an immediate increase of the singlet–triplet (ST_0 , where T_0 is middle triplet sublevel) mixed state population, which enhances the recombination of the singlet RP. The application of short MW pulse affords us satisfactory time resolution to observe its

effect dynamically. Recently, the ODESR at high magnetic field, Ku-band region, has been developed.^{5,6}

The time-resolved ODESR has been applied to the studies on spin dynamics of RPs in micellar solutions, because the RPs in micelles show large MFE due to their long lifetime by restriction of escape to bulk water. On the other hand, to the best of our knowledge, there has been no report on direct determination of their kinetic parameters except for the measurement of a radical ion pair (RIP) lifetime in 2-propanol by photoconductivity detected magnetic resonance,⁷ even though there have been many studies on MFEs of RPs and RIPs in homogeneous solutions.¹

The photoinduced electron-transfer reactions from zinc tetraphenyl porphyrin (ZnTPP) to quinones in homogeneous solution have been studied by Fourier transform and time-resolved ESR.^{8–15} The observed chemically induced dynamic electron spin polarization (CIDEP) spectra are mainly originated from triplet mechanisms (TM) and S– T_0 mixing radical pair mechanisms (ST_0 M-RPM).^{16,17} CIDEP due to ST_0 M-RPM is induced by the exchange interaction of the ST_0 mixed state at

* To whom correspondence should be addressed. E-mail: ysakaguc@riken.jp. Phone: +81-48-467-9395. Fax: +81-48-462-4664.

[†] Present address: Department of Chemistry, School of Science and Technology, Kwansai Gakuin University.

the re-encounter of the RP. The re-encounter of the ST_0 mixed state RP and the recombination of its singlet component are also an important processes in ODESER. Therefore it is interesting to compare the viscosity dependence of CIDEP and that of ODESER.

Furthermore, the CIDEP spectra of the RIPs at low temperature are attributed to not only TM and ST_0 M-RPM but the presence of spin correlated radical pairs (SCRPs),^{8–11} because it is thought that the RIPs are confined strongly by the Coulomb force. It is interesting to compare the formation and decay rates of the SCRPs signals to other kinetic parameters determined by the time-resolved ODESER.

In this paper, we investigated the spin dynamics of the RIP that formed in the photoinduced electron-transfer reaction from ZnTPP to 2-methyl-1,4-naphthoquinone (MNQ) in viscous alcohol solution by the X- (9.16 GHz) or Ku-band (17.41 GHz) ODESER. We observed the time profiles of the transient absorptions due to ZnTPP cation and MNQ anion radicals at 450 nm under the irradiation of the X- or Ku-band MW pulse at the resonant magnetic fields and the yields of the escaping radical ions with changing delay time to irradiate the MW pulse after laser excitation. From the analysis of these data, the important rate constants of the spin dynamics were determined at various solvent viscosities, and the viscosity dependence was investigated.

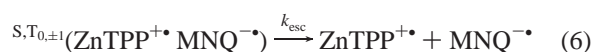
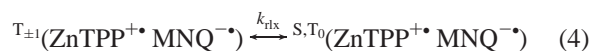
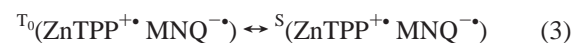
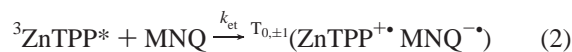
Experimental Section

MNQ, 2-propanol (2-PrOH) for high performance liquid chromatography, and cyclohexanol (c-HexOH) of guaranteed grade were purchased from Cica-Merck. ZnTPP was obtained from Acros. MNQ was purified by recrystallization from benzene. 2-PrOH, c-HexOH, and ZnTPP were used as received. The concentrations of ZnTPP and MNQ were 0.0002 and 0.002 M (mol dm⁻³), respectively, unless otherwise noted. The sample solutions were degassed under N₂ atmosphere and flowed into a quartz tube at 0.75 cm³/min and room temperature. The viscosities of mixtures of 2-PrOH and c-HexOH were measured by a viscometer (VM-1G-L, Yamaichi) and were about 5, 10, and 15 cP, corresponding to 2-PrOH:c-HexOH in volume = 1:1, 1:2, and 1:3, respectively. The dielectric constants of 2-PrOH, 20.18, and c-HexOH, 16.4, are similar to each other.¹⁸ The second harmonic, 532 nm, of an Nd:YAG laser (Quanta Ray GCR-3, Spectra-Physics or Precision II, Continuum) was used as an exciting light source. The measurement systems were similar to that described elsewhere.^{3,5} The MW fields, B_1 , were estimated from the relation between the MW power and the frequency of the quantum beat of escaping MNQ semiquinone radical from SDS micelle.^{5,19}

The cyclic voltammetry measurements were carried out using a potentiostat (HA-301, Hokuto Denko) controlled by a function generator (HB-111, Hokuto Denko) at room temperature under N₂ atmosphere. Pt wire, Pt coil, and Ag/Ag⁺ were used as working, counter, and reference electrodes, respectively. Tetra-*n*-butylammonium perchlorate (TBAP) was purchased from Cica-Merck and used as the supporting electrolyte. Its concentration was 0.06 M.

Results and Analysis

The photoinduced electron transfer from ZnTPP to MNQ in alcohol is considered to be same as those from ZnTPP to duroquinone (DQ) or benzoquinone (BQ).⁸ Thus the reaction scheme in the presence of magnetic field is shown as



Here ${}^{1,3}\text{ZnTPP}^*$ is the singlet or triplet excited state of ZnTPP, $\text{ZnTPP}^{+\bullet}$ is the ZnTPP cation radical, $\text{MNQ}^{-\bullet}$ is the MNQ anion radical, and $T_{0,\pm 1}$ and S are the spin states of the radical ion pair consisting of $\text{ZnTPP}^{+\bullet}$ and $\text{MNQ}^{-\bullet}$. Reactions 2–6 describe the photoinduced electron-transfer reaction (rate constant: k_{et}), the S– T_0 mixing, the spin–lattice relaxation (rate constant: k_{rlx}), the recombination of the singlet RP (rate constant: k_{rec}), and the escape process (rate constant: k_{esc}), respectively. The intersystem recombination that occurs from triplet RPs due to the spin–orbit coupling was neglected because it is effective in confined condition.²⁰

Parts a and b of Figure 1 exhibit transient absorption spectra of photoexcited ZnTPP (0.5 mM) in the absence and presence of MNQ (5 mM) in 2-PrOH, respectively. The peak and bleaching appeared at 450 and 660 nm, respectively. It is shown that the spectrum of ${}^3\text{ZnTPP}^*$ ²¹ at 7 μs after laser excitation was similar to that at 0.1 μs in Figure 1a. It has been known that the lifetime of ${}^3\text{ZnTPP}^*$ is very long.²² On the other hand, the intensity and shape of the spectrum due to photoexcited ZnTPP with MNQ at 7 μs were different from those at 0.1 μs as shown in Figure 1b. This is ascribed to the quenching of ${}^3\text{ZnTPP}^*$ and the appearance of radical ions. The peaks of the transient absorptions due to $\text{ZnTPP}^{+\bullet}$ and $\text{MNQ}^{-\bullet}$ appear at 409 nm in CH₂Cl₂²³ and at 403 nm in acetonitrile,²⁴ respectively. However, the light at wavelengths shorter than 440 nm is absorbed by the ground state of ZnTPP.²³ To avoid the deterioration of S/N ratio of the signal, we observed the time profiles of the transient absorption, $A(t)$, due to $\text{ZnTPP}^{+\bullet}$ and $\text{MNQ}^{-\bullet}$ at 450 nm in this study.

The irradiation of a resonant MW field enhances reaction 4. The populations of the $T_{\pm 1}$ state are generally larger than the ones of the ST_0 mixed state due to much slower relaxation than the recombination ($k_{\text{rec}} > k_{\text{rlx}}$). Consequently, the RIP is transferred from the $T_{\pm 1}$ states to the ST_0 mixed state by the resonant MW irradiation, irrespective of its bidirectional effect. Then the ST_0 mixed state vanishes quickly via the geminate recombination. Consequently, the yields of escape radical ions under MW irradiation decrease at resonant magnetic field. Figure 2 represents the ODESER spectrum due to the RIP consisting of $\text{ZnTPP}^{+\bullet}$ and $\text{MNQ}^{-\bullet}$. The vertical axis is the absorbance at 450 nm, which shows a stationary value at nonresonant conditions. On resonant condition such as at 326.9 mT, the yields of escaping $\text{ZnTPP}^{+\bullet}$ and $\text{MNQ}^{-\bullet}$ decrease and thus are observed as the decrease of the absorbance. The MW pulse of the width, $\Delta t_{\text{MW}} = 10 \mu\text{s}$, was irradiated at $t_{\text{D}} = -500 \text{ ns}$ after laser excitation with the MW field strength $B_1 = 0.04$ or 0.4 mT. The stick diagrams were simulated by the hyperfine coupling constants and g values of $\text{ZnTPP}^{+\bullet}$ ²³ and $\text{MNQ}^{-\bullet}$.^{25,26} The line width (fwhm = 1.0 mT) of ODESER spectrum at $B_1 = 0.04 \text{ mT}$ was similar to that of the stick diagrams. At $B_1 = 0.4 \text{ mT}$, the ODESER spectrum was broadened (fwhm = 2.2 mT), because RIP is transferred from the $T_{\pm 1}$ states to the ST_0 mixed state at even off-resonant magnetic field by the strong MW field.

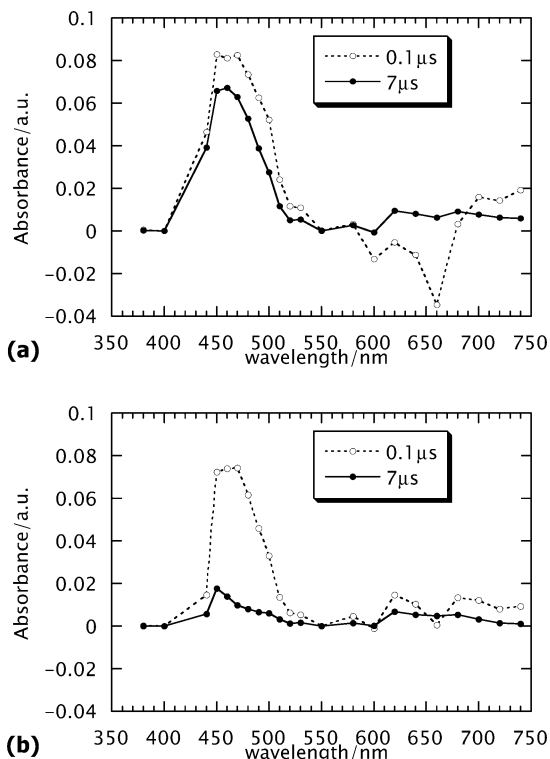


Figure 1. Transient absorption spectra of photoexcited ZnTPP (a) in the absence and (b) presence of MNQ in 2-PrOH at 0.1 and 7 μs after the laser excitation.

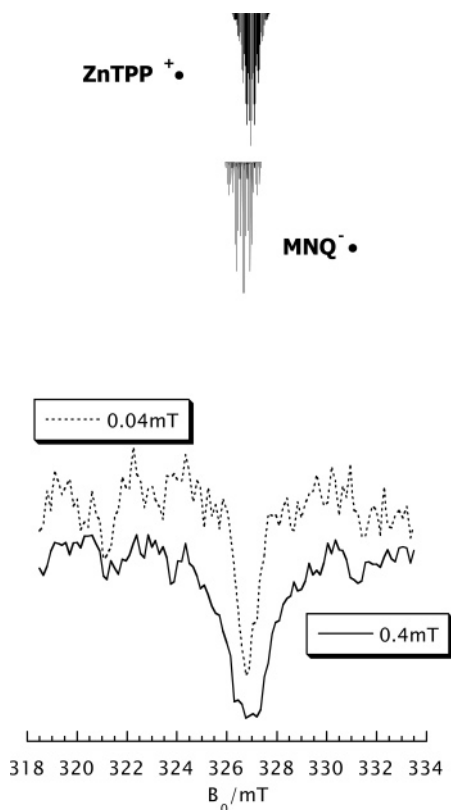


Figure 2. Simulated stick spectra and ODESR spectra, which were averaged $A(t)$ values from 10 to 18 μs after the laser excitation, observed by the photoinduced electron-transfer reaction between ZnTPP and MNQ in the mixture of 2-PrOH and *c*-HexOH at 15.2 cP.

The spin conversion by the irradiation of a resonant MW field proceeds only in its presence. This implies that we can induce the spin conversion much faster than the concerned reaction

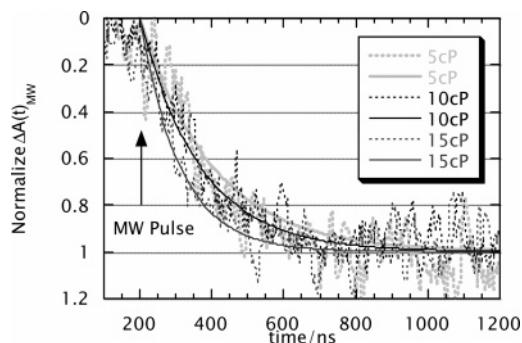


Figure 3. Differences in $A(t)$ curves due to the radical ions in the absence and presence of the X-band resonant microwave pulse, $\Delta A(t)_{\text{MW}}$. These are plotted against the time after laser excitation. The microwave pulse was irradiated at 200 ns. The curves are normalized to each other. The dotted and solid curves show the experimental and fitting results, respectively.

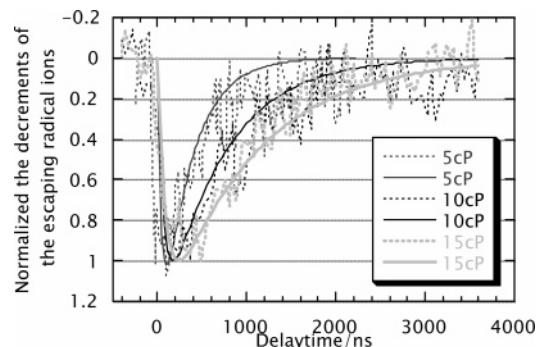


Figure 4. Differences in the yields of the escaping radical ions, which were averaged $A(t)$ values from 10 to 18 μs after the laser pulse, between in the absence and presence of the X-band resonant microwave pulse. These are plotted against the delay time to irradiate the microwave pulse after the laser excitation, t_D . The curves are normalized to each other. The dotted and solid curves show the experimental and fitting results, respectively.

kinetics by applying a short resonant MW pulse. Thus, we can observe the change of following reaction dynamically, which we call the “single-pulse response”. Figure 3 shows the differences between $A(t)$ values in the absence and presence of a single X-band MW π -pulse with $\Delta t_{\text{MW}} = 40$ ns, $t_D = 200$ ns, and $B_1 = 0.4$ mT. The difference appeared more quickly at the higher viscosity. In the “single-pulse response” experiment, the MW pulse transfers the population from that in the $T_{\pm 1}$ states to that in the ST_0 mixed state in Δt_{MW} without changing the sum. The population in the ST_0 mixed state, however, decreases much faster than that in the $T_{\pm 1}$ states. Consequently, the above difference decays with the rate constant of k_{MS} , which can be written as

$$k_{\text{MS}} = k_{\text{rec}}/2 + k_{\text{esc}} + k_{\text{rlx}} \quad (7)$$

If the Δt_{MW} is short enough compared to $1/k_{\text{MS}}$, we can observe the decay as shown in Figure 3.

The effect of resonant MW irradiation is proportional to the population difference between $T_{\pm 1}$ states and the ST_0 mixed state, $[T_{\pm 1}] - [ST_0]$. If we observe this MW effect by shifting the irradiation time with reference to the initiation of the reaction (i.e., laser irradiation), we can observe the population difference at the moment of the MW irradiation. We call this technique the “pulse-shift measurement”. Figure 4 expresses the decrements of the escaping radical ions due to the X-band MW pulse ($\Delta t_{\text{MW}} = 40$ ns, $B_1 = 0.4$ mT) with shifting the MW irradiation time after laser excitation, $t_D = -0.4$ to 3.6 μs . The curve rose

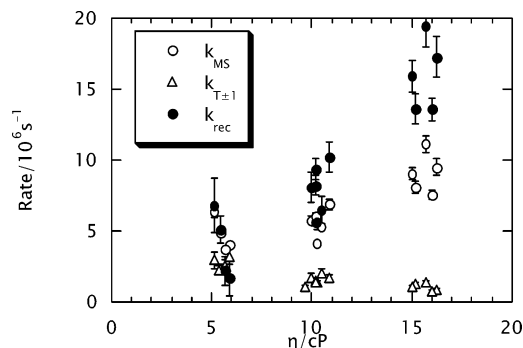


Figure 5. Dependence of the geminate recombination rates (filled circles) and decay rates of the $T_{\pm 1}$ and ST_0 mixed states (open triangles and circles, respectively) on the solvent viscosity.

and fell slower as the viscosity became higher. The maximum decrement due to MW pulse was enlarged increasing the viscosity.

Since $[T_{\pm 1}]$ and $[ST_0]$ grow together with the formation of RIP via the photoinduced electron-transfer reaction, $[T_{\pm 1}] - [ST_0]$ increases with the pseudo-first-order electron-transfer rate, $k_{et}[\text{MNQ}]$, except for $[T_{\pm 1}] = [ST_0]$. The decay rate of the ST_0 mixed state, k_{MS} , contributes to the increase of $[T_{\pm 1}] - [ST_0]$, because it can be assumed that only $[ST_0]$ decreases with k_{MS} in the early stage after laser excitation. Therefore the rise of $[T_{\pm 1}] - [ST_0]$ consists of two components: the pseudo-first-order electron-transfer rate, k_{et} , and k_{MS} .

At larger delay times, $[T_{\pm 1}] - [ST_0]$ is equal to $[T_{\pm 1}]$ because the ST_0 mixed state becomes very low due to the fast recombination. Thus the decay of $[T_{\pm 1}] - [ST_0]$ is determined mostly by the decrease in $[T_{\pm 1}]$. The decay rate of the $T_{\pm 1}$ states, $k_{T_{\pm 1}}$, is given by following equation

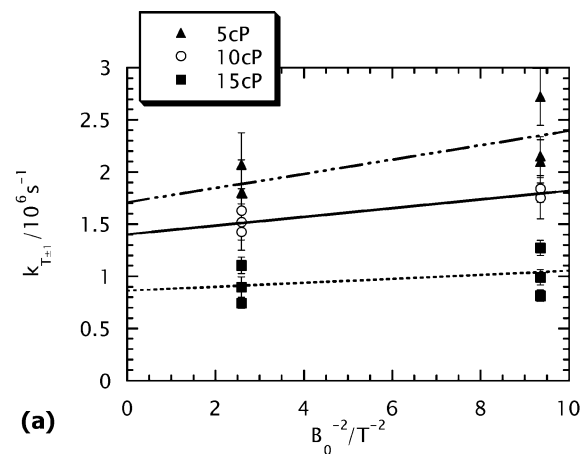
$$k_{T_{\pm 1}} = k_{\text{esc}} + k_{\text{rlx}} \quad (8)$$

We estimated the values of k_{et} and $k_{T_{\pm 1}}$ by the fitting of the rise and decay of the curves as shown in Figure 4, respectively.

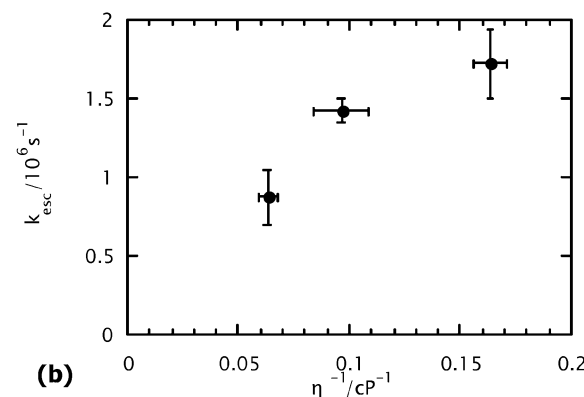
Discussion

In Figure 5, k_{rec} , $k_{T_{\pm 1}}$, and k_{MS} values are plotted against the solvent viscosities, η . The values of k_{rec} are estimated by $2(k_{MS} - k_{T_{\pm 1}})$. In the present study, k_{rec} is approximately proportional to η . It has been reported that the geminate recombination rates of MNQ semiquinone (MNQH $^{\bullet}$) and SDS alkyl radicals in the SDS micelle are (15 ± 2) and $(11 \pm 2) \times 10^6 \text{ s}^{-1}$ at $t_D = 0.3$ and $2.5\text{--}3.5 \mu\text{s}$, respectively.³ The microviscosity of SDS micelle has been reported to be 8.3 cP by the ^{13}C spin–lattice relaxation time²⁷ or 16.5 cP by the fluorescence polarization.²⁸ The decrease of k_{rec} at later t_D or smaller η observed in this experiment is qualitatively rationalized by decrease in the existence probability of the partner radical in the reaction volume due to the diffusion.

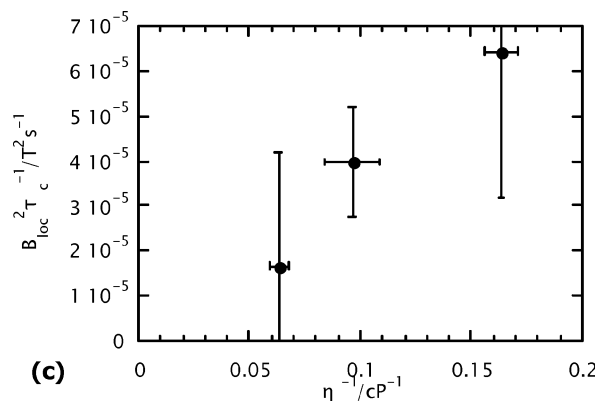
Figure 6a exhibits the decay rates of $T_{\pm 1}$ states, $k_{T_{\pm 1}}$, which depend on the external magnetic fields. These values were determined by the “pulse-shift technique” using X ($B_0 = 326.9$ mT, $B_1 = 0.4$ mT, $\Delta t_{\text{MW}} = 40$ ns) and Ku bands ($B_0 = 621.2$ mT, $B_1 = 0.11$ mT, $\Delta t_{\text{MW}} = 6 \mu\text{s}$). In the Ku-band, the long MW pulse was turned on t_D after laser irradiation. Under this condition, only the decay curve corresponding to lifetime of $T_{\pm 1}$ was observed.²⁹ The external magnetic field dependence is originated from the spin–lattice relaxation. Under high magnetic fields, the spin–lattice relaxation rate in the absence of g anisotropy is given by



(a)



(b)



(c)

Figure 6. (a) The decay rates of the $T_{\pm 1}$ states that are plotted against the inverse square of the external magnetic field, B_0^{-2} . (b) Dependence of the escape rates on the solvent viscosity. (c) Dependence of the B_{loc}^2/τ_c ($k_{\text{rlx}}B_0^2$) on the solvent viscosity.

$$k_{\text{rlx}} = \frac{\tau_c \gamma^2 B_{\text{loc}}^2}{1 + \tau_c^2 \gamma^2 B_0^2} \approx \frac{B_{\text{loc}}^2}{\tau_c B_0^2} \quad (9)$$

where τ_c is the rotational correlation time, γ is the electron gyromagnetic ratio, B_{loc} is the anisotropy of hyperfine coupling constants to induce the spin–lattice relaxation, and B_0 is the external magnetic field. The extrapolated values of $k_{T_{\pm 1}}$ at $B_0^{-2} = 0$ are free from relaxation and are equal to k_{esc} . The slopes in Figure 6a are within the expectation of the linear dependence on B^2 .

The values of k_{esc} and B_{loc}^2/τ_c are roughly in inverse proportion to η as shown in parts b and c of Figure 6, respectively. They are rationalized by the Stokes–Einstein–Debye equations for translational and rotational diffusions

$$D = k_B T / 6\pi\eta R \quad (10)$$

and

$$\tau_c = 4\pi\eta R^3 / 3k_B T \quad (11)$$

respectively. Here R is molecular radius. $1/k_{\text{esc}}$ is the time to separate RIP into escaping radical ions and proportional to η . Since the unit of D is m^2/s , $(D/k_{\text{esc}})^{1/2}$ has the dimension of distance, and the dependences on η cancel each other. If we regard this value as the maximum distance between the component radical ions of RIP, it seems constant at a certain dielectric constant, i.e., irrespective of viscosity.

The anomalous small escape rate of RIP consisting of the xanthone anion and N,N' -diethylaniline cation radicals in 2-propanol, $4 \times 10^6 \text{ s}^{-1}$, has been already reported by Matsuyama et al.⁷ They thought that the reason is the property of the 2-propanol and Coulomb interaction. However, the simple continuum diffusion model explained the viscosity dependence of the kinetic parameters in this experiment. Therefore the slow escape process may be caused by the long distance to separate RIP into escaping radical ions. Freed and Pedersen have studied the CIDEP due to $\text{ST}_0\text{M-RPM}$, and ascribed the origin of its polarization to the exchange interaction in the re-encountering RPs and defined the lifetime of the encounter pair, τ_1 , as follows³⁰

$$\tau_1 = \frac{d}{\alpha D} \left(1 + \frac{1}{\alpha d} \right) \quad (12)$$

where d is a distance of the closest approach, and α is an exponential decay constant in the inter-radical distance, r , for the exchange interaction, $J(r)$, given by

$$J(r) = J_0 \exp[-\alpha(r - d)] \quad (13)$$

Thus the lifetime of the encounter pair strongly depends on α . In the condition of a large α (20 nm^{-1}), the experimental $\text{ST}_0\text{M-RPM}$ polarization of the neutral RPs in homogeneous solution has been reproduced by the calculation.^{31,32} Thus the neutral RPs feel J at a short distance, where solvent structure and molecular interaction influence re-encounter of the neutral RPs.^{31,32} However, the α has been reported to be a small value around 10 nm^{-1} (i.e., slower decay) in the system of RPs.³³ The RPs live longer than the neutral RPs and feel J at long distances, where the Coulomb and other interaction are negligible. Therefore the simple diffusion model has also been adopted for the analysis of the CIDEP due to $\text{ST}_0\text{M-RPM}$.³³

SCRIP consists of the radicals that interact with each other via J . The decay rate of SCRIP produced by photoinduced electron transfer from ZnTPP to BQ in 2-butanol at room temperature, 3.1 cP,¹⁸ is reported to be $3.6 \times 10^6 \text{ s}^{-1}$.¹¹ This value is similar to the decay rate of $\text{T}_{\pm 1}$ states RIP consisting of $\text{ZnTPP}^{+\bullet}$ and $\text{MNQ}^{-\bullet}$ observed by the X-band ODESr at 5 cP, $k_{\text{T}_{\pm 1}} = (2.3 \pm 0.4) \times 10^6 \text{ s}^{-1}$. Thus the SCRIP lifetime is explained in terms of the relaxation and escape process.

In Figure 7, the pseudo-first-order electron-transfer rates are plotted against η^{-1} . The values of $k_{\text{et}}[\text{MNQ}]$ are roughly proportional to η^{-1} , because the electron-transfer reaction is diffusion controlled reaction and depends on the encounter frequency of donor and acceptor molecules. This result is consistent with the viscosity dependence of the pseudo-first-order rates of formation of BQ anion radical via the photoinduced electron transfer from zinc 5,10,15,20-tetra(4-sulfonatophe-

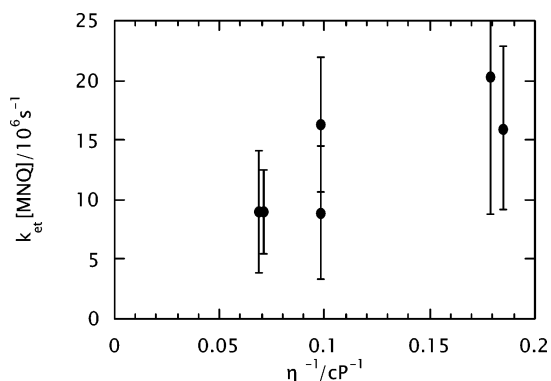


Figure 7. Dependence of the pseudo-first-order electron-transfer rates on the solvent viscosity.

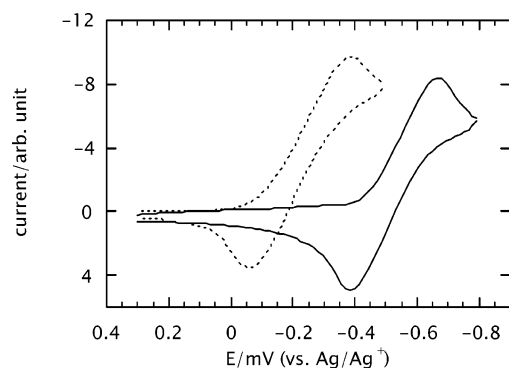


Figure 8. Cyclic voltammogram of 0.002 M BQ (dotted curve) and 0.002 M MNQ (solid curve) observed with scan rate of 20 mV s^{-1} in mixed alcohol, 2-PrOH:c-HexOH in volume = 1:1, containing 0.06 M TBAP.

nyl)-21*H*,23*H*-porphine (ZnTPPS) to BQ in water and ethanol mixed solution.¹²

The second-order electron-transfer rates also depend on the acceptor concentration.^{13,34} Even if we take the concentration dependence into account, the value of k_{et} from ZnTPP to MNQ at 5 cP, $10^{10} \text{ M}^{-1} \text{ s}^{-1}$ at $[\text{MNQ}] = 2 \times 10^{-3} \text{ M}$, is much larger than those to BQ in 2-butanol at room temperature ($\eta = 3.1 \text{ cP}$), $2.2 \times 10^9 \text{ M}^{-1} \text{ s}^{-1}$ at $[\text{BQ}] = 10^{-2} \text{ M}$,^{10,11} and $2.7 \times 10^9 \text{ M}^{-1} \text{ s}^{-1}$ at $[\text{BQ}] = 3 \times 10^{-3} \text{ M}$.¹⁵ In the electron-transfer reaction, one of the important parameter is Gibbs energy, ΔG , which is simply expressed by³⁵

$$\Delta G = E_{\text{ox}} - E_{\text{red}} - E_{\text{T}} \quad (14)$$

where E_{ox} is the oxidation potential of ZnTPP, E_{red} are the reduction potentials of quinones, and E_{T} is the triplet energy of ZnTPP. When the ΔG is negative, the electron-transfer reaction occurs smoothly. Figure 8 shows the cyclic voltammogram of BQ and MNQ. The values of E_{red} determined from the midpoints between the cathodic and anodic peak potentials. The E_{red} for BQ was larger than the E_{red} for MNQ. The same trend was observed in 2-butanol and benzonitrile containing 0.06 M TBAP. The ΔG for BQ is smaller than the ΔG for MNQ, whereas the electron-transfer reaction from ZnTPP to BQ is slower than that to MNQ. In the Marcus normal region, the smaller ΔG becomes, the larger the electron-transfer reaction rate becomes. Therefore the reaction potentials of the triplet precursor and the RIP consisting of $\text{ZnTPP}^{+\bullet}$ and BQ anion radical may cross in the Marcus inverted region.^{36,37}

Conclusion

The kinetic parameters of the RIP consisting of $\text{ZnTPP}^{+\bullet}$ and $\text{MNQ}^{-\bullet}$ at various solvent viscosities (5, 10, and 15 cP) were

determined by the X- and Ku-band ODESR using short MW pulses. The geminate recombination, the escape, the relaxation, and the pseudo-first-order electron-transfer rates strongly depend on the solvent viscosity as: (1) $k_{\text{rec}} \propto \eta$; (2) $k_{\text{esc}} \propto \eta^{-1}$; (3) under high magnetic fields, $k_{\text{rx}} \propto \eta^{-1}$; and (4) $k_{\text{et}}[\text{MNQ}] \propto \eta^{-1}$. Thus these kinetic parameters of the RIP in homogeneous solution obey the simple continuum diffusion model.

The comparison between the viscosity dependence of the kinetic parameters of the RIPs and that of the neutral RPs is noteworthy. The former is explained by the simple diffusion model because the effective ST₀M-RPM polarization distance is long enough.³³ However, ST₀M-RPM polarization of the neutral RPs has been reproduced by assuming the solvent structure and molecular interaction because of the short effective CIDEP distance.^{31,32}

Acknowledgment. This work has been carried out under Special Postdoctoral Researchers Program and the Molecular Ensemble Project of RIKEN. The authors are greatly indebted to Dr. M. Kawai, Head of the Surface Chemistry Laboratory in RIKEN, for her continuing encouragement. Y.K. is very grateful to Dr. Y. Kobori for fruitful discussion on the ST₀M-RPM polarization distance.

References and Notes

- (1) Steiner, U. E.; Ulrich, T. *Chem. Rev.* **1989**, *89*, 51.
- (2) Hayashi, H. *Photochemistry and Photophysics*; CRC Press: Boca Raton, 1990; Vol. 1, p 59.
- (3) Sakaguchi, Y.; Astashkin, A. V.; Tadjikov, B. M. *Chem. Phys. Lett.* **1997**, *280*, 481.
- (4) Woodward, J. R.; Sakaguchi, Y. *J. Phys. Chem. A* **2001**, *105*, 4010.
- (5) Sakaguchi, Y. *Mol. Phys.* **2002**, *100*, 1129.
- (6) Kitahama, Y.; Sakaguchi, Y. *Mol. Phys.* **2002**, *100*, 1451.
- (7) Matsuyama, A.; Maeda, K.; Murai, H. *J. Phys. Chem.* **1999**, *103*, 4137.
- (8) van Willigen, H.; Levstein, P. R.; Ebersole, M. H. *Chem. Rev.* **1993**, *93*, 173.
- (9) Kroll, G.; Plüschau, M.; Dinse, K.-P.; van Willigen, H. *J. Chem. Phys.* **1990**, *93*, 8709.
- (10) Yamauchi, S.; Ueda, T.; Satoh, M.; Akiyama, K.; Tero-Kubota, S.; Ikegami, Y.; Iwaizumi, M. *J. Photochem. Photobiol., A* **1992**, *65*, 177.
- (11) Hirota, N.; Yamauchi, S. *Dynamic Spin Chemistry*; Kodansha: Tokyo, 1998; pp 233–234.
- (12) Ebersole, M. H.; van Willigen, H. *Z. Phys. Chem.* **1993**, *182*, 89.
- (13) Ebersole, M. H.; Levstein, P. R.; van Willigen, H. *J. Phys. Chem.* **1992**, *96*, 9310.
- (14) Plüschau, M.; Zahl, A.; Dinse, K. P.; van Willigen, H. *J. Chem. Phys.* **1989**, *90*, 3153.
- (15) Iwaizumi, M.; Yamamoto, K.; Ohba, Y.; Yamauchi, S. *Coord. Chem. Rev.* **1994**, *132*, 29.
- (16) Muus, L. M.; Atkins, P. W.; McLauchlan, K. A.; Pedersen, J. B. *Chemically Induced Magnetic Polarization*; Reidel: Dordrecht, 1977.
- (17) Murai, H.; Hayashi, H. *Radiation Curing in Polymer Science and Technology*; Elsevier Applied Science: London and New York, 1993; Vol. 2, p 63.
- (18) Lide, D. R. *Handbook of Chemistry and Physics 77th Edition*; CRC Press: Boca Raton, 1996; Chap. 6–151 and Chap. 6–208.
- (19) Tadjikov, B. M.; Astashkin, A. V.; Sakaguchi, Y. *Chem. Phys. Lett.* **1998**, *283*, 179.
- (20) Khudyakov, I. V.; Serebrennikov, Y. A.; Turro, N. J. *Chem. Rev.* **1993**, *93*, 537.
- (21) Pekkarinen, L.; Linschitz, H. *J. Am. Chem. Soc.* **1960**, *82*, 2407.
- (22) Fujisawa, J.; Ohba, Y.; Yamauchi, S. *J. Am. Chem. Soc.* **1997**, *119*, 8736.
- (23) Fajer, J.; Borg, D. C.; Forman, A.; Dolphin, D.; Felton, R. H. *J. Am. Chem. Soc.* **1970**, *92*, 3451.
- (24) Amada, I.; Yamaji, M.; Tsunoda, S.; Shizuka, H. *J. Photochem. Photobiol., A* **1996**, *95*, 27.
- (25) Dodd, N. J. F.; Mukherjee, T. *Biochem. Pharmacol.* **1984**, *33*, 379.
- (26) Pedersen, J. A. *Handbook of EPR spectra from quinones and quinols*; CRC Press: Boca Raton, 1985.
- (27) Menger, F. M.; Jerkunica, J. M. *J. Am. Chem. Soc.* **1978**, *100*, 688.
- (28) Fujiwara, Y.; Taga, Y.; Tomonari, T.; Akimoto, Y.; Aoki, T.; Tanimoto, Y. *Bull. Chem. Soc. Jpn.* **2001**, *74*, 237.
- (29) Konishi, Y.; Okazaki, M. *Appl. Magn. Reson.* **1998**, *14*, 131.
- (30) Freed, J. H.; Pedersen, J. B. *Adv. Magn. Reson.* **1976**, *8*, 1.
- (31) Tominaga, K.; Yamauchi, S.; Hirota, N. *J. Chem. Phys.* **1990**, *92*, 5175.
- (32) Kitahama, Y.; Kimura, Y.; Hirota, N. *Bull. Chem. Soc. Jpn.* **2000**, *73*, 851.
- (33) Kobori, Y.; Yago, T.; Tero-Kubota, S. *Appl. Magn. Reson.* **2003**, *23*, 269.
- (34) Stevens, B. *Chem. Phys. Lett.* **1987**, *134*, 519.
- (35) Rehms, D.; Weller, A. *Israel J. Chem.* **1970**, *8*, 259.
- (36) Marcus, R. A. *J. Chem. Phys.* **1956**, *24*, 966.
- (37) Marcus, R. A. *Annu. Rev. Phys. Chem.* **1964**, *15*, 155.